ACS BIO & MED CHEM Au
AN OPEN ACCESS JOURNAL OF THE AMERICAN CHEMICAL SOCIETY

pubs.acs.org/biomedchemau

Article

Immunomodulatory Bandage for Accelerated Healing of Diabetic Wounds

Jayashree Vijaya Raghavan, Vinod Kumar Dorai, Shruthi Ksheera Sagar, Archana Sivaraman, Kalpana S R, and Siddharth Jhunjhunwala*

Cite This: *ACS Bio Med Chem Au* 2022, 2, 409–418

Read Online

ACCESS | Metrics & More | Article Recommendations | Supporting Information

ABSTRACT: Diabetic foot ulcers are challenging to treat. Current strategies to treat these wounds focus on preventing infection and promoting tissue regrowth but are ineffective in many individuals. Low-grade chronic inflammation is present in individuals with diabetes, and altering the inflammatory responses at the wound site could be an alternate approach to promote healing. We hypothesized that immunomodulation of the wound microenvironment would result in accelerated healing. To test this hypothesis, we began by characterizing the changes in the myeloid cell phenotype in a mouse model [leptin receptor knockout (KO) mouse] that closely mimics the type 2 diabetes condition observed in humans. We observed increased numbers of monocytes and neutrophils in the circulation of the KO mice compared to that in wild-type control mice. We also observed several phenotypic changes in neutrophils from the KO diabetic mice, suggesting low-grade systemic inflammation. Hence, we developed a rapamycin-loaded chitosan scaffold that may be used to modulate immune responses. The use of these immunomodulatory scaffolds at a wound site resulted in accelerated healing compared to the healing using blank scaffolds. In summary, our data suggest that immunomodulation may be a viable strategy to promote the healing of wounds in individuals with diabetes.

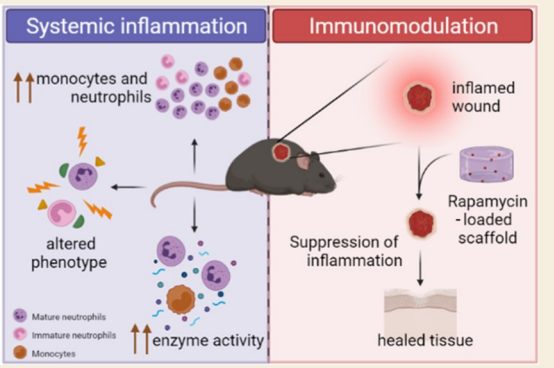

KEYWORDS: *chronic wounds, diabetic foot ulcers, diabetes, inflammation, immunomodulation, rapamycin, healing*

INTRODUCTION

Individuals with diabetes are at a risk of developing several complications, one of which is the formation of foot ulcers. Diabetic foot ulcers (DFUs) are chronic wounds that are challenging to treat,[1,2] and 25−40% of wounds fail to heal despite receiving the current standard of care.[3−5] The lack of healing leads to gangrene formation in a significant proportion of individuals, necessitating limb amputation.[6,7]

DFUs show delayed healing due to a compromised microvasculature, peripheral neuropathy, and dysregulated wound healing,[8−10] and hence, most treatment strategies under development attempt to address these issues. However, a few reports suggest that chronic low-grade systemic inflammation, which is present in individuals with diabetes,[11,12] may also play a role in delaying wound healing.[13−15] Low-grade systemic inflammation may lead to altered recruitment and an increased presence of myeloid cells (monocytes and neutrophils) at the wound site,[16,17] an increased M1/M2 ratio,[18] and increased extracellular matrix degeneration,[19] each of which have been observed in human and animal models of diabetic chronic wounds. Additionally, an increased presence of neutrophil extracellular trap components in diabetic wounds has been shown to cause delayed healing, and inhibition of trap formation enhances wound healing.[20−22] Together, these observations suggest that monocytes and neutrophils in circulation and at the wound site have a vital role to play in the induction and sustenance of inflammation in diabetic wounds.

Hence, we hypothesized that modulating the inflammatory microenvironment at the wound site would promote healing in diabetic wounds. To test this hypothesis, here, we begin by characterizing the monocyte and neutrophil phenotype in a leptin receptor knockout ($LepR^{-/-}$) mouse, which become diabetic at ∼8 weeks of age.[23] We show that the knockout (KO) mice have increased numbers of both monocytes and neutrophils in circulation and that the circulatory neutrophils have activation deficits. Hence, we developed and tested the efficacy of an immunomodulatory drug-releasing bandage on the healing of surgical wounds in KO mice. Our bandages showed accelerated healing, which was comparable to wild-type (WT) non-diabetic animals. These observations suggest that modu-

Received: December 8, 2021
Revised: March 19, 2022
Accepted: March 22, 2022
Published: April 4, 2022

lation of inflammation in diabetic wounds has the potential to improve healing outcomes.

METHODS

Animal Ethical Approval

All animal experiments were performed in accordance with the ethical approval from the Institutional Animal Ethics Committee, Indian Institute of Science (CAF/Ethics/546/2017) under the Control and Supervision Rules, 1998 of the Ministry of Environment and Forest Act (Government of India). Leptin receptor heterozygous ($LepR^{-/+}$) animals were purchased from The Jackson Laboratory (strain—B6.BKS(D)-Leprdb/J), Bar Harbor, Maine, USA and bred at the Central Animal Facility, Indian Institute of Science. Homozygous KO animals were found to be obese between 4 and 8 weeks and diabetic by 8−10 weeks of age. KO animals aged 14−22 weeks were used for experiments along with their littermate (age-matched) WT animals serving as controls.

Genotyping

Tail snips were collected from all animals between 6 and 10 weeks of age. The tail snips were digested with 600 μL of sodium chloride-Tris-ethylenediaminetetraacetic acid (EDTA) buffer containing 20 μL of proteinase K (Thermo Fisher Scientific, USA) and incubated in a water bath maintained at 65 °C for 5−6 h. Minced samples were centrifuged at a 10,000 relative centrifugal force (RCF) for 10 min at room temperature. The supernatant was washed with isopropanol followed by 70% ethanol, and the resultant pellet was dried at room temperature for 1 h. The pellet containing the DNA was suspended in 1× Tris-EDTA buffer, and the total DNA content was quantified using a NanoDrop 1000 spectrophotometer (Thermo Fisher Scientific). Polymerase chain reaction for amplification of the gene of interest was performed using primers (Merck, USA) recommended by the supplier and an EmeraldAmp GT PCR Master Mix (Takara Bio Inc., USA). Restriction digestion of the amplicons was performed using RSAI (Thermo Fisher Scientific). The digested samples were run on a 3% agarose gel along with a DNA ladder, and WT, heterozygous, and homozygous KO mice were identified as those that presented a single band at 135, two bands at 135 and 108, and a single band of 108 base pairs, respectively.

Sample Collection

Blood and bone marrow were retrieved from WT and KO animals for performing immunophenotyping and functional assays. Briefly, the animals were first anaesthetized using an intramuscular injection of a ketamine and xylazine mix. About 1 mL of blood was collected retro-orbitally, and animals were euthanized immediately. The femur and tibia were collected for isolating bone marrow cells. The isolated cells were passed through a 100 μm sterile-steel mesh to remove debris and centrifuged at 4 °C for 4 min at 400 RCF. RBC lysis was performed using 1 mL of the lysis buffer for 5 min at room temperature and quenched using 10 mL of 1× PBS. The samples were washed and suspended in 1 mL of 1× PBS for counting using a hemocytometer. Parallelly, blood samples were subjected to RBC lysis at 1:10 (blood to lysis buffer) by volume for 10 min at room temperature and quenched with 20 mL of 1× PBS. The samples were washed and resuspended in 1 mL of 1× PBS for counting. Both the samples were counted manually using a Bright-Line hemocytometer (0.1 mm) (Hausser Scientific, USA).

Immunophenotyping Using Flowcytometry

After counting, 2×10^5 blood and bone marrow cells were suspended in 500 μL of 1× PBS and were subjected to activation using 5 μg/mL cytochalasin B (Merck) for 7 min at 37 °C followed by 5 μM fMLP (Merck) stimulation at 37 °C for 30 min. Another set of samples without stimulation served as non-activated controls. The cells were then washed and stained with BD Horizon Fixable Viability Stain 510 to stain the dead cells. Following one washing step, the cells were suspended in the staining buffer containing the antibodies mentioned in Table S1. After staining for 30 min, the samples were washed and suspended in 300 μL of the staining buffer and run through a flow cytometer (BD FACSCelesta Cell Analyzer, BD Biosciences, USA). Single color controls were prepared using compensation beads (BD CompBeads, BD Biosciences) according to the manufacturer's instruction and used for compensation at the time of data analyses. Fluorescence-minus-one control for each color was prepared to correct for the group effect of a fluorophore on spectral spill. Voltages were set on a system using BD FACSDiva CS&T Research Beads (BD Biosciences) to correct for voltage-induced changes in median fluorescence intensity (MFI) across days of sample acquisition. A minimum of 20,000 $CD45^+$ live events for blood samples and 30,000 $CD45^+$ live events for bone marrow samples were acquired using a BD FACSDiva Version 6 Software system (BD Biosciences).

Myeloperoxidase and Elastase Activity Assay

White blood cells (2×10^5) and bone marrow cells (1×10^6) were seeded in triplicate in 96-well flat-bottom plates. One set of samples were stimulated with 5 μg/mL cytochalasin B for 7 min at 37 °C, washed, and followed by 5 μM fMLP stimulation at 37 °C for 30 min. Separately, two sets of samples were subjected to the same processing conditions without stimulation. One of the non-stimulated samples was subjected to 0.5% cetyltrimethylammonium bromide treatment for 15 min at 37 °C to measure the total enzyme activity upon cell lysis. The plates were centrifuged at 4 °C for 10 min, and the supernatant was stored at −80 °C.

Myeloperoxidase (MPO) enzyme activity in the supernatant was measured using 3,3′,5,5′-tetramethylbenzidine (Merck, USA), which was mixed and incubated for 90 s. The reaction was quenched using an equal volume of 1 M H_2SO_4 to arrest the reaction. Absorbance at 450 nm was measured along with standard samples (range 26−1333 mU/mL) prepared using human MPO (Merck, USA). The MPO activity of the samples was measured by interpolation from a standard curve.

Similarly, elastase activity was measured using a 1 mM methoxysuccinyl-Ala-Ala-Pro-Val *p*-nitroanilide (Merck) substrate. Absorbance at 405 nm was measured continuously for 60 min from the time of substrate addition along with standard samples (range 16−166 IU/mL) prepared using human elastase (Merck).

Scaffold Fabrication and Characterization

Chitosan scaffolds were prepared as described with slight modifications to the protocol.[24] Briefly, 1% chitosan gel was prepared by dissolving chitosan in deionized water containing 1% acetic acid under a continuous stirring condition for 48 h. The gel was centrifuged at 3350 RCF to pellet-undissolved chitosan flakes, and a clear supernatant was used for scaffold fabrication. The gel was aliquoted by weight (750 or 2000 mg) in 5 or 10 mL scintillation vials, respectively. Rapamycin (1 or 50 μg) or tetracycline (10 or 100 μg) was added to make drug-loaded scaffolds. The samples were vortexed thoroughly and frozen at −80 °C for a minimum of 3 h. The samples were lyophilized for 48 h using a freeze-dryer (TAITEC, Japan). Sterile crosslinked scaffolds were prepared by treating the lyophilized gels with 1 mL of sterile 5% tripolyphosphate (Merck) at pH 5 for 5 min followed by two washes using sterile 1× PBS.

To determine the swelling characteristics, tripolyphosphate crosslinked scaffolds were weighed and immersed in 2 mL of 1× PBS and kept at 37 °C. At various times, the weight of the scaffold was measured after approximately 5 min of drying to remove excess water. Following weighing, the scaffolds were immersed in freshly replenished 1× PBS. The change in weight at every time point was determined by normalizing the value to the original weight of the scaffold.

Atomic Force Microscopy

Crosslinked scaffolds (blank and drug-loaded) were subjected to liquid mode atomic force microscopy (Park Systems, South Korea) using a soft tip cantilever (radius of curvature, 2600 nm). Force−displacement ($F-D$) measurements were performed by randomly choosing 5−10 points per scaffold. The recorded $F-D$ curves were analyzed using XEI software (Park Systems) using a Hertzian model to calculate Young's modulus.

https://doi.org/10.1021/acsbiomedchemau.1c00063
ACS Bio Med Chem Au 2022, 2, 409−418

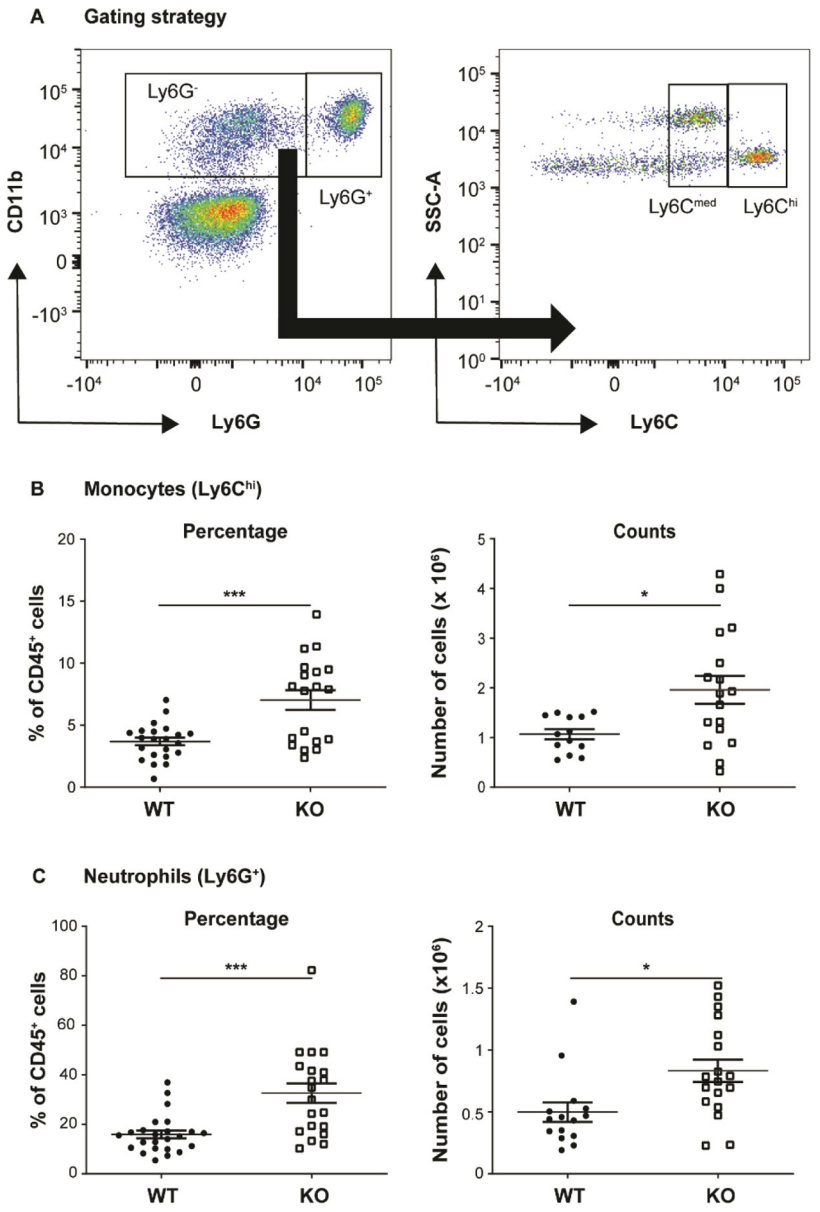

Figure 1. Circulating monocyte and neutrophil numbers. (A) Gating strategy used to identify neutrophils ($CD45^+CD11b^+Ly6G^+$) and monocytes ($CD45^+CD11b^+Ly6G^-Ly6C^+$). Two sub-populations of monocytes were identified based on the Ly6C expression as $Ly6C^{med}$ and $Ly6C^{hi}$. (B,C) Circulating percentages (left panel) and counts (right panel) of monocytes and neutrophils in WT and KO mice. $N \geq 13$ per group pooled from at least six different independent experiments. A Student's *t*-test was performed to determine the significance. * indicates a p value < 0.05 and *** indicates a p value < 0.001.

Drug Release Kinetics

Crosslinked scaffolds were submerged in 2 mL of 1× PBS containing 1% sodium dodecyl sulfate in 1× PBS for rapamycin release or 1 mL of 1× PBS for tetracycline release and incubated at 37 °C. At different times, the solution was removed and saved at −20 °C. The wells were replenished with same volumes of respective buffers. The concentration of rapamycin and tetracycline in the frozen supernatants was determined by reading the absorbance at 278 and 360 nm, respectively (at room temperature) and compared to a standard curve generated by measuring the absorbance of the free drug at different concentrations.

Surgical Wounding

The animals were anesthetized using 5% isoflurane in a gas anesthesia system (Orchid Scientific, India). The dorsal portion of the body was shaved, and the surgical area was sterilized by an alternate application of betadine and isopropanol three times. A splinted wound healing model was created, as described.[25] Briefly, silicone splints of 0.5 mm thickness (Grace Bio-Labs, USA) of size 1.2 cm × 1.2 cm with an internal diameter of 8 mm was cut using an 8 mm biopsy punch. The splints were ethanol-sterilized and adhered to the skin on the dorsum on either side of the midline using a strong-bonding cyanoacrylate adhesive (Loctite 495, Germany). Skin excision was performed by cutting along the circular margins of the splint to create a 7 mm full-thickness dermal wound. Wounds were imaged using 48 MP digital camera along with a physical ruler. A scaffold or gauze was placed on the wounds and held firmly using clear semi-occlusive dressing (3M Tegaderm, USA). The animals were injected with buprenorphine (0.05 mg/kg body weight) just before surgery and 18 h post-surgery. Food paste and water were provided on the cage floor for 3 days to help with recovery from surgical stress. The wounds were followed for 20 days thereafter, and the dressing was changed every 3−4 days. Wound images were analyzed using ImageJ software by manual tracing of wound edges. The calculated wound area was divided by the original wound area (on day 0) to calculate the percentage of healing.

https://doi.org/10.1021/acsbiomedchemau.1c00063
ACS Bio Med Chem Au 2022, 2, 409−418

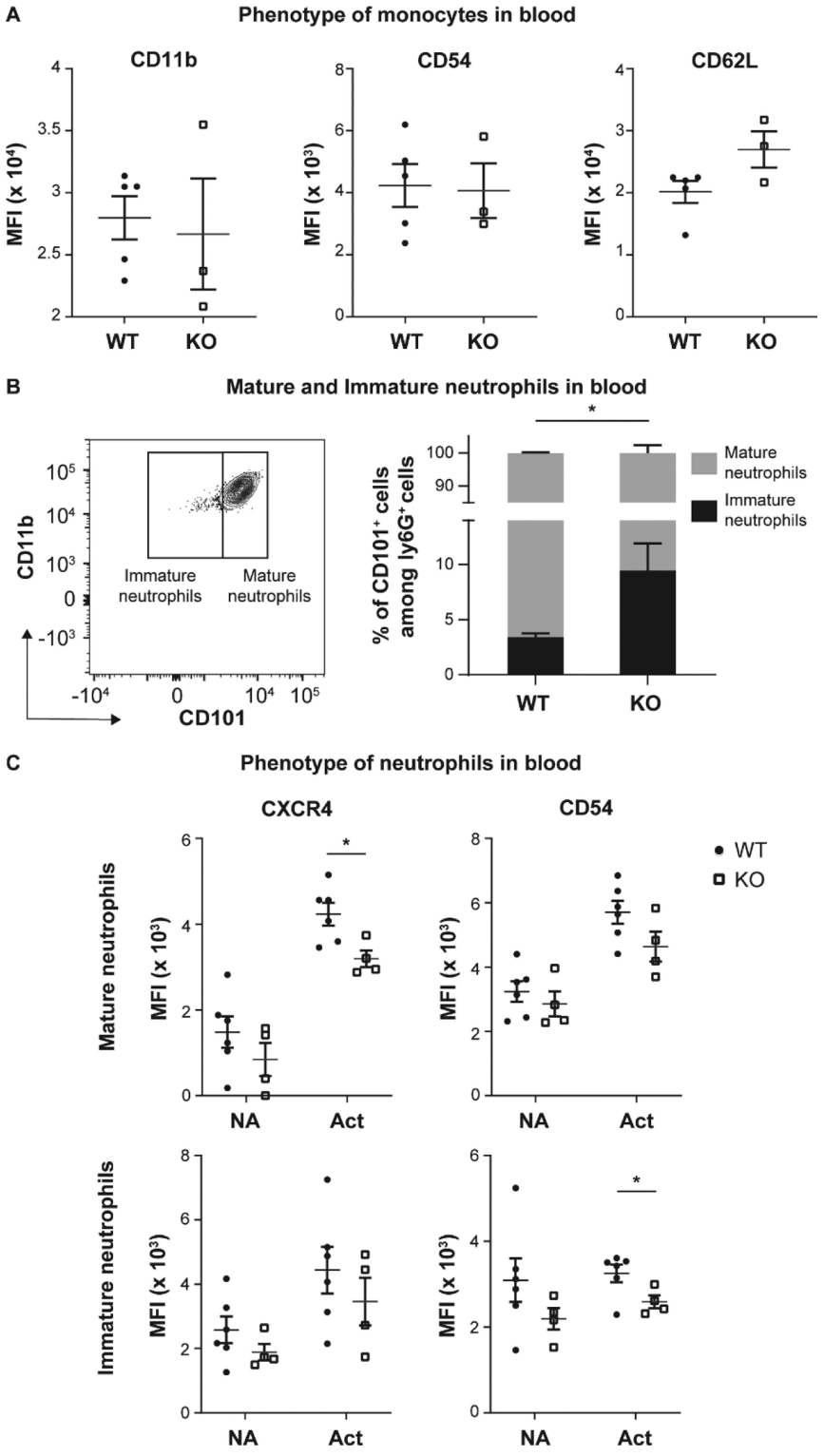

Figure 2. Phenotype of circulating monocytes and neutrophils. (A) Comparison of surface protein expression CD11b, CD54, and CD62L on circulating monocytes ($Ly6C^{hi}$) between WT and KO mice. (B) Gating strategy (left panel) to measure immature neutrophil ($CD101^{-}$ among $CD11b^{+}Ly6G^{+}$) percentages, and its quantification (right panel) in WT and KO mice. (C) Expression of CXCR4 and CD54 among non-activated (NA) and activated (Act) mature and immature neutrophils from WT and KO mice. $N \geq 3$ mice per group pooled from at least three different independent experiments. A Student's *t*-test was performed to determine the significance. * indicates a p value <0.05.

Statistics

Data presented are based on three or more independent experiments with a total of at least three animals in each group. Two-tailed Student's *t*-test was used for comparing two groups. Two-way ANOVA with Tukey's test for multiple comparisons was used for multiple group comparison. Wound healing data were analyzed by performing multiple group comparisons at every time point. The significance is represented as $*p < 0.05$, $**p < 0.01$, $***p < 0.001$, and $****p < 0.0001$. All data are presented as mean ± standard deviation.

https://doi.org/10.1021/acsbiomedchemau.1c00063
ACS Bio Med Chem Au 2022, 2, 409−418

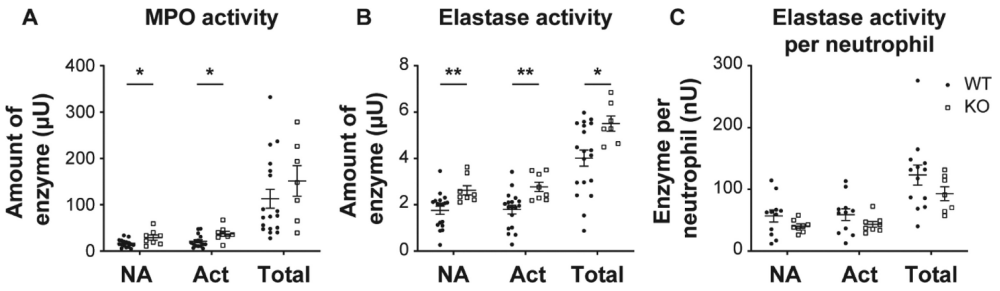

Figure 3. Activity of neutrophil extracellular trap-associated enzymes MPO and elastase in circulating white blood cells. (A,B) *Ex vivo* measurement of MPO (A) and elastase (B) among all circulating white blood cells under non-activating (NA) and activating (Act) conditions, or whole cell measurement (total), in WT and KO mice. (C) Normalized elastase activity when normalization was performed by dividing the elastase activity value by the number of neutrophils present among the circulating white blood cells. $N \geq 7$ per group pooled from at least five different independent experiments. A Student's *t*-test was performed to determine the significance. * indicates a p value <0.05 and ** indicates a p value <0.01.

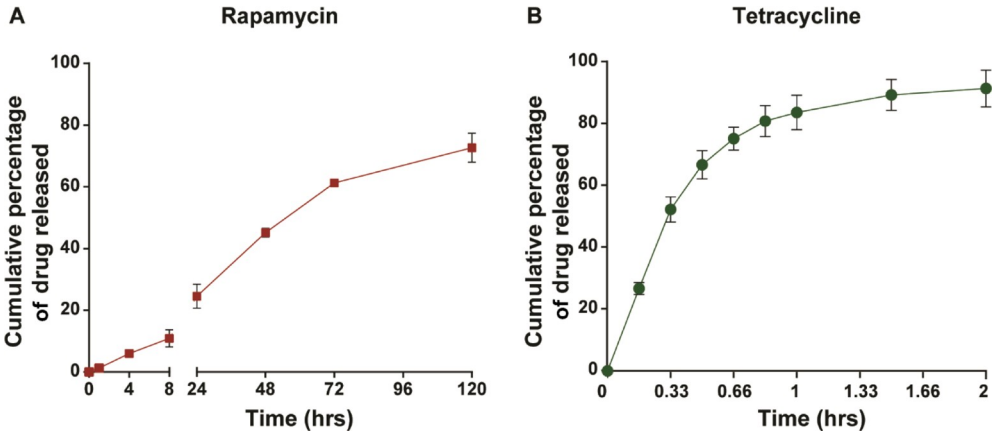

Figure 4. *In vitro* release kinetics of rapamycin and tetracycline. (A,B) Release of rapamycin (50 μg initial loading) or tetracycline (100 μg initial loading) was measured over time, and the percentage released is plotted. $N = 3$ per group.

RESULTS

Circulating Immune Cells in Diabetic Mice

We began by assessing the changes in frequencies of immune cells in circulation as chronic low-grade systemic inflammation is known to be present in obese mice,[26,27] such as the leptin receptor KO diabetic mice. This specific mouse model is considered to be a good representation of diabetic wounds and in many ways resembles diabetes in humans.[25,28] Immune cells were identified as $CD45^+$ live cells, and among these cells, neutrophils were identified as $Ly6G^+$ and monocytes as $Ly6C^{hi}$ (Figure 1A). Among the cells in the blood, we observed a significantly higher percentage and number of monocytes (Figure 1B) and neutrophils (Figure 1C) in KO mice compared to WT littermates. The increased percentages of both these cell populations correlated with a decreased percentage in B cells, but no changes in the percentages of $Ly6C^{med}$, CD4, and CD8 expressing T cells were observed (Figure S1).

Phenotype of Monocytes and Neutrophils in the Blood and Bone Marrow

Next, we characterized the phenotype of monocytes and neutrophils from the KO mice. Among circulating monocytes ($Ly6C^{hi}$), the expressions of the standard cell−surface proteins, such as integrin and selectin (CD11b, CD54, and CD62L), were not different in KO and WT mice (Figure 2A). Among circulating neutrophils, we observed a significant decrease in CD101-expressing cells in KO compared to WT mice (Figure 2B), suggesting that a significant proportion of these cells were immature.[29] Additionally, the circulating neutrophils showed a lowered ability to upregulate the expression of the cell-surface proteins CXCR4 and CD54 following activation (Figure 2C), which are key molecules involved in neutrophil migration and recruitment. We also assessed the ability of the circulating white blood cells to secrete two key enzymes, MPO and elastase, that are essential for fighting invading pathogens and could play a role in wound healing.

Ex vivo cultures of circulating immune cells from KO mice showed increased secretion of both MPO and elastase under non-activating and activating conditions compared to cells from WT mice (Figure 3A,B). Total cellular activity of elastase was also higher (Figure 3B), but we observed that the increased secretion was likely a result of increased number of neutrophils in circulation. That is, the amount of secreted elastase per neutrophil was not significantly different between the KO mice and cells of WT mice (Figure 3C).

A similar analysis was performed for cells in the bone marrow. No differences were observed among monocytes and the number of CD101-expressing neutrophils between the KO and WT mice (Figures S2A,B). However, the ability of bone marrow neutrophils to increase the expression of CXCR4 following activation was compromised (Figure S2C), and the overall *ex vivo* activity of elastase protein in these cells was also lower in KO mice as compared to WT mice (Figure S2D).

Together, these observations suggest that the phenotype and potential activity of neutrophils are altered at a systemic level in diabetic mice, which may affect their functions at a wound site, causing delayed healing. Hence, we hypothesized that delivery of

https://doi.org/10.1021/acsbiomedchemau.1c00063
ACS Bio Med Chem Au 2022, 2, 409−418

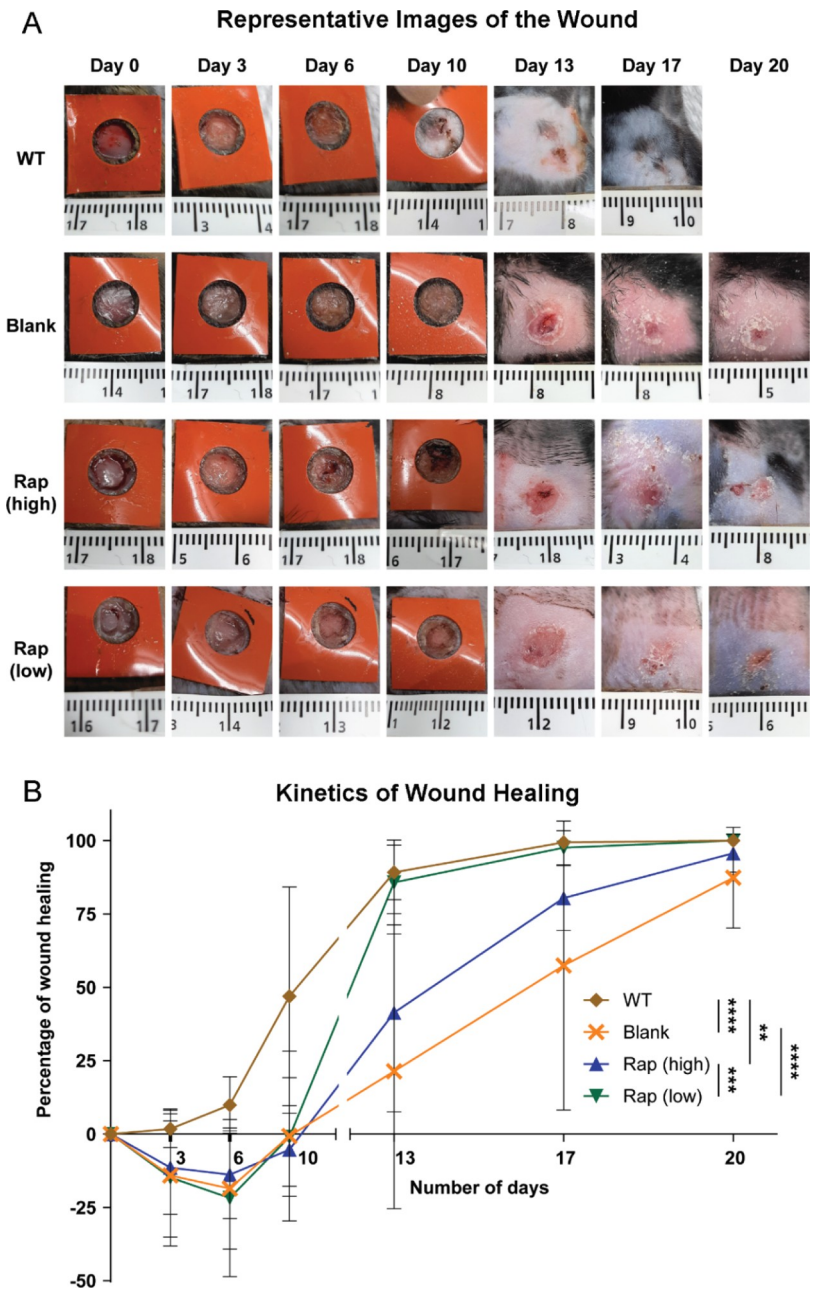

Figure 5. Wound healing in KO (diabetic) and WT mice. (A) Representative wound images for each group over 20 days are shown. (B) Percentage change in the wound area is plotted over time. Data are representative of multiple wounds, with $N \geq 4$ animals per group pooled from at least four independent experiments. Two-way ANOVA with Tukey's test for multiple comparisons was performed to determine the statistical significance. The statistical significance observed at day 13 is shown next to the legend, and ** indicates a p value < 0.01, *** indicates a p value < 0.001, and **** indicates a p value < 0.0001.

an agent that broadly modulates immune cell activity may assist in accelerating wound healing.

Drug-Loaded Scaffolds for Application on Wounds

Chitosan-based scaffolds and bandages are commonly used in wound-healing applications.[30] Hence, we used chitosan scaffolds for our studies. The scaffolds were prepared using a simple freeze-drying procedure using cylindrical molds. As wound sites are known to secrete a large amount of fluid, we tested if the as-prepared chitosan scaffolds would be stable in aqueous solutions. When placed in aqueous solutions, we observed that the chitosan scaffolds would swell and break apart quickly (Figure S3A). Hence, tripolyphosphate crosslinking was performed to improve the chitosan scaffolds' mechanical stability in aqueous solutions, and we observed that they did not fall apart easily (Figure S3A). A scanning electron micrograph of the crosslinked scaffold is shown in Figure S3B. Upon exposure to aqueous solutions, the crosslinked scaffolds increased their weight by 4.93-fold but remained stable thereafter for 4 days in the same aqueous solution (Figure S3C). Additionally, the crosslinked scaffolds (with drug encapsulated inside them) had a Young's modulus that was comparable to that of the skin (Figure S3D).

Next, we loaded two different drugs into these formulations and assessed their release. Rapamycin was chosen due to its immunomodulatory properties,[31,32] and tetracycline was chosen

https://doi.org/10.1021/acsbiomedchemau.1c00063
ACS Bio Med Chem Au 2022, 2, 409−418

as it is an antibiotic with potential anti-inflammatory properties. *In vitro* release measurements showed that about 60−75% of rapamycin released within 3−5 days (Figure 4A), while ∼80% of tetracycline was released within 2 h (Figure 4B). A slower release of rapamycin is expected due to its relatively larger molecular weight. The timeframe of rapamycin release (3−5 days) was well-suited for application in diabetic wounds, as bandages are commonly changed every 2−3 days in the clinic.[33] Having established that the chitosan scaffolds had desirable mechanical properties and could be used for topical drug release, we next assessed their ability to heal wounds in the diabetic mouse model.

Rapamycin Accelerates Wound Closure in LepR$^{-/-}$ Diabetic Mice

We used a splinted skin wound model to test the ability of our scaffolds to accelerate wound healing. These wounds are known to heal within 2 weeks in WT mice, but the healing is delayed in diabetic mice and occurs over 3−4 weeks.[34] We tested two different drug doses (1 and 50 μg for rapamycin; 10 and 100 μg for tetracycline) for each drug and determined their ability to promote wound healing compared to that of drug-free (blank) scaffolds. Representative images of wounds from each treatment group from the day of wounding (day 0) till complete healing (day 20) are shown in Figure 5A. Quantitative assessment of healing was performed by calculating the percentage reduction in wound area, which is shown in Figure 5B. We observed that the application of chitosan scaffolds loaded with a low dose of rapamycin resulted in accelerated wound healing compared to the blank (in KO mice), which was most apparent at day 13 post wounding (Figure 5B). However, a high dose of rapamycin did not significantly increase the rate of wound healing compared to the blank, which could be attributed to the anti-proliferative properties of the drug in addition to immunomodulatory properties. Histopathological analysis of skin sections appeared to correlate with the wound closure data at day 13. Using hematoxylin and eosin staining (Figure S4A), reepithelization, granulation tissue, inflammatory cell infiltrates, and fibroblast numbers were determined, and through Masson's trichrome staining (Figure S4B), collagen fiber orientation was assessed by a pathologist. However, statistical analysis was not performed due to the low number of histological sections. Further, we observed that low-dose rapamycin-loaded scaffolds were better at accelerating wound healing than the tetracycline-loaded scaffolds, which by themselves were slightly better than the blank scaffolds in increasing the rate of wound healing (Figure S5). Together, these results indicate that an immunomodulatory drug-loaded scaffold has the potential to accelerate healing of diabetic wounds.

DISCUSSION

Wound healing is a complex process that involves crosstalk among various cellular and molecular players that bring about a tightly coordinated action of wound closure. Generally, it may be thought to progress through three phases: initial inflammation, cellular proliferation, and tissue remodeling.[10] However, in chronic wounds, this coordinated cascade of events is dysregulated.[10,15] In diabetes, it is thought that cellular proliferation and tissue remodeling are stalled, possibly due to infection. Hence, most treatment strategies in the clinic focus on clearing the dead tissue through debridement, removal of the wound exudate, and moisture control through frequent dressing changes, application of antibiotics for infection control, and growth factor ointments for enhanced proliferation and accelerated wound closure.[14,35,36] Newer treatment strategies currently under development also focus on clearance of infection, promoting angiogenesis (neovascularization), and re-epithelialization.[37,38] However, many of these strategies do not appear to work on a significant number of individuals with DFUs. In this context, it is being recognized that chronic inflammation is present in individuals with diabetes. Consequently, the switch from inflammation to cellular proliferation may not occur in the healing cascade, resulting in delayed wound closure.[10,13,15] Hence, we hypothesized that immunomodulation at the site of diabetic wounds would help reduce the local inflammation, accelerating wound healing.

To test any immunomodulatory system we developed, we needed to use a preclinical animal model. The leptin receptor KO mouse model is regarded as a good representation of type-2 diabetes, and hence we chose it for our studies.[39] To understand the status of immune cells, specifically the myeloid cells that play essential roles in wound healing, in these diabetic mice, we characterized their number and phenotype (Figures 1−3). We observed an increased percentage and numbers of both monocytes and neutrophils in circulation in the diabetic mice compared to WT mice (Figure 1), similar to an observation made in individuals with type 2 diabetes by Zhang and colleagues.[40] We also observed an increased number of immature neutrophils in the circulation of diabetic mice (Figure 2), which usually occurs during active and sustained inflammation that causes a reduction in the maturation time of these cells in the bone marrow.[41,42] Additionally, these mice show deficits in the upregulation of CXCR4 post-activation (Figure 2). CXCR4 is required for reverse migration of neutrophils to the bone marrow from circulation.[43] It has been suggested that aged neutrophils under inflammatory conditions begin to increase the CXCR4 expression for their return to the bone marrow and clearance by bone marrow macrophages.[44] A deficit in the upregulation of CXCR4 post-activation may affect this function, which needs further investigation.

Myeloid cells, specifically neutrophils, secrete granular proteins and enzymes such as MPO and elastase as part of neutrophil extracellular traps (NETs) to fight infections. These enzymes and NET structures may also hinder wound healing.[45] We observed that circulating immune cells from diabetic mice had a higher activity of both MPO and elastase enzymes under non-activated and activated conditions (Figure 3). While the per neutrophil enzyme activity was not higher in diabetic mice than in WT mice, as we observe a greater number of these cells in circulation and others have observed a higher number[46] and prolonged presence in wounds,[47] increased enzyme activity at the wound site is likely.[45] Additionally, neutrophil elastase has been observed to correlate with poor healing in patients with chronic wounds, suggesting that an increased enzyme activity could be detrimental for wound healing.[21] Together, the data shown in Figures 2 and 3 showing alterations in neutrophil and possibly monocyte phenotype supported our hypothesis that delivery of immunomodulatory drugs at the wound site would reduce inflammation and thereby improve healing, a concept that has been suggested by others too.[48]

While the idea of modulating immune responses to reduce inflammation and hence promote healing is not necessarily new, its application in diabetic wounds has been limited due to the possibility of increasing the risk of infection. One recent example of such an approach is the use of an annexin A1 mimetic peptide

https://doi.org/10.1021/acsbiomedchemau.1c00063
ACS Bio Med Chem Au 2022, 2, 409−418

drug (Ac2-26) to promote healing by resolving inflammation.[49] However, in this study, several different components were included in the wound dressing, making it quite complex. Further, the aforementioned drug does not directly counteract infections. In our study, we focused on making the bandage simpler and utilizing a single molecule that could function both as an immunomodulator and as an antibiotic.

Hence, the immunomodulatory drug we chose was rapamycin, which is both an immunomodulator and an antibiotic, and hence could play the dual role of modulating the inflammatory response[32] while also preventing bacterial and fungal infections.[50] We also chose another drug, tetracycline, which is a well-known antibiotic and has been suggested to have anti-inflammatory properties. Several different controlled release formulations of these molecules have been previously synthesized.[31] As chitosan-based bandages are commonly used in diabetic wounds,[30] our goal was to determine if direct encapsulation and release of the drugs was possible from these chitosan bandages. As we demonstrate through studies on release kinetics (Figure 4), while it was possible to release rapamycin over a 3−5 day period, most of the tetracycline was released within 2 h, possibly due to the differences in their molecular weights. We did not add additional barriers to slow down the release (such as encapsulating in nano- or microparticles) as we aimed to keep the bandage as simple as possible.

One of the study's limitations is that we do not yet understand the exact mechanisms of rapamycin action on immune cells at the local wound site that result in accelerated healing. We speculate that rapamycin, through its action on the mammalian target of rapamycin-regulated immune responses,[32] may be acting in several ways. It has been suggested that rapamycin blocks the granulocyte macrophage colony-stimulating factor-induced migration of neutrophils.[51] The drug also reduces the hyper-responsive states of neutrophils following severe injury[52] and has been shown to inhibit NET formation in activated neutrophils.[53] Rapamycin is also known to affect monocyte and macrophage polarization and suppress the production of chemokines that recruit innate and adaptive immune cells.[32,54] Together, rapamycin affects several features of innate immune cell function, including migration, cytokine production, and polarization.[32] Hence, the rapamycin scaffolds may be accelerating healing by altering the migration patterns and activity of innate immune cells that are normally observed in large numbers in chronic diabetic wounds. Interestingly, we observe that a low dose of rapamycin accelerated wound healing but not a high dose of the drug or the blank scaffold (Figure 5). This observation of inverse-dose-dependent change in healing outcome could be attributed to the anti-proliferative property of rapamycin,[55,56] which might reduce the proliferation of fibroblasts, epithelial cells, and endothelial cells, thereby slowing the wound healing process. We speculate that an optimum dose of rapamycin is required for suppressing inflammation while not preventing cellular proliferation, which could be the low dose used by us. Additionally, at this low dose, the action of the drug is likely only topical.

Another limitation of the study is that while we demonstrate that the crosslinked chitosan scaffolds swell rapidly in the presence of aqueous solutions but maintain their overall structure, we do not measure the equilibrium water content or the water vapor transmission rate[57] from these scaffolds. The latter two properties are important for the design of scaffolds that ensure that an optimal amount of moisture remains at the wound site to promote healing, and it requires further investigation in the future. Further, we used a wounding model known to show contraction-based wound healing, which does not mimic the natural wound healing observed in humans. Although we used splints to avoid contraction-based healing in mice, after 13 days of wounding, we consistently observed a certain degree of contraction-based healing leading to wound closure by 3 weeks. Before clinical translation, our results on wound closure will need to be tested in other models of wounding that do not heal due to contraction.

CONCLUSIONS

We show that in leptin receptor KO mice, which are commonly used for preclinical studies on diabetes, circulating monocytes and neutrophils have an increased frequency and altered activation phenotype. These changes in myeloid cells have been linked to slower healing of wounds in diabetic mice. Hence, we developed an immunomodulatory drug releasing scaffold with the express purpose of promoting wound healing in these diabetic mice. We demonstrate that the rapamycin-loaded chitosan scaffolds result in accelerated healing of wounds when compared to blank scaffolds. Such scaffolds have the potential to be used in the clinic to improve healing of DFUs.

ASSOCIATED CONTENT

Supporting Information

The Supporting Information is available free of charge at https://pubs.acs.org/doi/10.1021/acsbiomedchemau.1c00063.

> Immune cell percentages in blood, myeloid cell phenotype in the bone marrow, scaffold characterization, histopathology of skin tissue, and tetracycline-loaded scaffold-based healing data (PDF)

AUTHOR INFORMATION

Corresponding Author

Siddharth Jhunjhunwala − *Centre for BioSystems Science and Engineering, Indian Institute of Science, Bengaluru, Karnataka 560012, India*; orcid.org/0000-0001-8046-2288; Email: siddharth@iisc.ac.in

Authors

Jayashree Vijaya Raghavan − *Centre for BioSystems Science and Engineering, Indian Institute of Science, Bengaluru, Karnataka 560012, India*

Vinod Kumar Dorai − *Centre for BioSystems Science and Engineering, Indian Institute of Science, Bengaluru, Karnataka 560012, India*

Shruthi Ksheera Sagar − *Centre for BioSystems Science and Engineering, Indian Institute of Science, Bengaluru, Karnataka 560012, India*

Archana Sivaraman − *Centre for BioSystems Science and Engineering, Indian Institute of Science, Bengaluru, Karnataka 560012, India*

Kalpana S R − *Sri Jayadeva Institute of Cardiovascular Sciences and Research, Bengaluru, Karnataka 560069, India*

Complete contact information is available at: https://pubs.acs.org/10.1021/acsbiomedchemau.1c00063

Notes

The authors declare no competing financial interest.

ACKNOWLEDGMENTS

The central animal facility at IISc is acknowledged for its support with all our experiments. We thank Giri Gaonkar and Rakshith for their help with breeding of animals and Khader, Sunitha, and Pooja for assistance with genotyping. We acknowledge Alakesh for his assistance with experiments involving animals. This work was primarily funded by the Science and Engineering Board, Department of Science and Technology, Government of India grant (ECR/2016/000629) to S.J. S.J. is a recipient of the Intermediate Fellowship (IA/I/19/1/504265) from the DBT/Wellcome Trust India Alliance programme.

ABBREVIATIONS

DFUs	diabetic foot ulcers
KO	knockout
$LepR^{-/-}$	leptin receptor KO
MPO	myeloperoxidase
NET	Neutrophil Extracellular Trap
Rap	rapamycin (only in figure)
RCF	relative centrifugal force
WT	wild type

REFERENCES

(1) Frykberg, R. G.; Banks, J. Challenges in the Treatment of Chronic Wounds. *Adv. Wound Care* **2015**, *4*, 560−582.
(2) Jeffcoate, W. J.; Vileikyte, L.; Boyko, E. J.; Armstrong, D. G.; Boulton, A. J. M. Current Challenges and Opportunities in the Prevention and Management of Diabetic Foot Ulcers. *Diabetes Care* **2018**, *41*, 645−652.
(3) Prompers, L.; Schaper, N.; Apelqvist, J.; Edmonds, M.; Jude, E.; Mauricio, D.; Uccioli, L.; Urbancic, V.; Bakker, K.; Holstein, P.; Jirkovska, A.; Piaggesi, A.; Ragnarson-Tennvall, G.; Reike, H.; Spraul, M.; Van Acker, K.; Van Baal, J.; Van Merode, F.; Ferreira, I.; Huijberts, M. Prediction of Outcome in Individuals with Diabetic Foot Ulcers: Focus on the Differences between Individuals with and without Peripheral Arterial Disease. The EURODIALE Study. *Diabetologia* **2008**, *51*, 747−755.
(4) Guest, J. F.; Ayoub, N.; McIlwraith, T.; Uchegbu, I.; Gerrish, A.; Weidlich, D.; Vowden, K.; Vowden, P. Health Economic Burden That Wounds Impose on the National Health Service in the UK. *BMJ Open* **2015**, *5*, No. e009283.
(5) Boulton, A. J. M.; Armstrong, D. G.; Kirsner, R. S.; Attinger, C. E.; Lavery, L. A.; Lipsky, B. A.; Mills, J. L.; Steinberg, J. S. Diagnosis and Management of Diabetic Foot Complications. *Diabetes* **2018**, *2018*, 1−20.
(6) Jeffcoate, W. J.; Chipchase, S. Y.; Ince, P.; Game, F. L. Assessing the Outcome of the Management of Diabetic Foot Ulcers Using Ulcer-Related and Person-Related Measures. *Diabetes Care* **2006**, *29*, 1784−1787.
(7) Boulton, A. J. M. The Pathway to Foot Ulceration in Diabetes. *Med. Clin.* **2013**, *97*, 775−790.
(8) Dinh, T.; Veves, A. Microcirculation of the Diabetic Foot. *Curr. Pharm. Des.* **2005**, *11*, 2301−2309.
(9) Chao, C. Y. L.; Cheing, G. L. Y. Microvascular Dysfunction in Diabetic Foot Disease and Ulceration. *Diabetes/Metab. Res. Rev.* **2009**, *25*, 604−614.
(10) Wilkinson, H. N.; Hardman, M. J. Wound Healing: Cellular Mechanisms and Pathological Outcomes. *Open Biol.* **2020**, *10*, 200223.
(11) Pickup, J. C.; Crook, M. A. Is Type II Diabetes Mellitus a Disease of the Innate Immune System? *Diabetologia* **1998**, *41*, 1241−1248.
(12) Hotamisligil, G. S. Inflammation and Metabolic Disorders. *Nature* **2006**, *444*, 860−867.
(13) Bannon, P.; Wood, S.; Restivo, T.; Campbell, L.; Hardman, M. J.; Mace, K. A. Diabetes Induces Stable Intrinsic Changes to Myeloid Cells That Contribute to Chronic Inflammation during Wound Healing in Mice. *Dis. Models Mech.* **2013**, *6*, 1434−1447.
(14) Baltzis, D.; Eleftheriadou, I.; Veves, A. Pathogenesis and Treatment of Impaired Wound Healing in Diabetes Mellitus: New Insights. *Adv. Ther.* **2014**, *31*, 817−836.
(15) Wicks, K.; Torbica, T.; Mace, K. A. Myeloid Cell Dysfunction and the Pathogenesis of the Diabetic Chronic Wound. *Semin. Immunol.* **2014**, *26*, 341−353.
(16) Ochoa, O.; Torres, F. M.; Shireman, P. K. Chemokines and Diabetic Wound Healing. *Vascular* **2007**, *15*, 350−355.
(17) Joshi, N.; Pohlmeier, L.; Ben-Yehuda Greenwald, M.; Haertel, E.; Hiebert, P.; Kopf, M.; Werner, S. Comprehensive characterization of myeloid cells during wound healing in healthy and healing-impaired diabetic mice. *Eur. J. Immunol.* **2020**, *50*, 1335−1349.
(18) Krzyszczyk, P.; Schloss, R.; Palmer, A.; Berthiaume, F. The Role of Macrophages in Acute and Chronic Wound Healing and Interventions to Promote Pro-Wound Healing Phenotypes. *Front. Physiol.* **2018**, *9*, 419.
(19) Huang, Y.; Kyriakides, T. R. The Role of Extracellular Matrix in the Pathophysiology of Diabetic Wounds. *Matrix Biol. Plus* **2020**, *6*−*7*, 100037.
(20) Wong, S. L.; Demers, M.; Martinod, K.; Gallant, M.; Wang, Y.; Goldfine, A. B.; Kahn, C. R.; Wagner, D. D. Diabetes Primes Neutrophils to Undergo NETosis, Which Impairs Wound Healing. *Nat. Med.* **2015**, *21*, 815−819.
(21) Fadini, G. P.; Menegazzo, L.; Rigato, M.; Scattolini, V.; Poncina, N.; Bruttocao, A.; Ciciliot, S.; Mammano, F.; Ciubotaru, C. D.; Brocco, E.; Marescotti, M. C.; Cappellari, R.; Arrigoni, G.; Millioni, R.; Vigili de Kreutzenberg, S.; Albiero, M.; Avogaro, A. NET osis Delays Diabetic Wound Healing in Mice and Humans. *Diabetes* **2016**, *65*, 1061−1071.
(22) Kaur, T.; Dumoga, S.; Koul, V.; Singh, N. Modulating Neutrophil Extracellular Traps for Wound Healing. *Biomater. Sci.* **2020**, *8*, 3212−3223.
(23) Coleman, D. L. Obese and Diabetes: Two Mutant Genes Causing Diabetes-Obesity Syndromes in Mice. *Diabetologia* **1978**, *14*, 141−148.
(24) Silvestro, I.; Francolini, I.; Di Lisio, V.; Martinelli, A.; Pietrelli, L.; Scotto d'Abusco, A.; Scoppio, A.; Piozzi, A. Preparation and Characterization of TPP-Chitosan Crosslinked Scaffolds for Tissue Engineering. *Materials* **2020**, *13*, 3577.
(25) Michaels, J.; Churgin, S. S.; Blechman, K. M.; Greives, M. R.; Aarabi, S.; Galiano, R. D.; Gurtner, G. C. db/dbmice exhibit severe wound-healing impairments compared with other murine diabetic strains in a silicone-splinted excisional wound model. *Wound Repair Regen.* **2007**, *15*, 665−670.
(26) Hotamisligil, G. S.; Shargill, N. S.; Spiegelman, B. M. Adipose Expression of Tumor Necrosis Factor-α: Direct Role in Obesity-Linked Insulin Resistance. *Science* **1993**, *259*, 87−91.
(27) Xu, H.; Barnes, G. T.; Yang, Q.; Tan, G.; Yang, D.; Chou, C. J.; Sole, J.; Nichols, A.; Ross, J. S.; Tartaglia, L. A.; Chen, H. Chronic Inflammation in Fat Plays a Crucial Role in the Development of Obesity-Related Insulin Resistance. *J. Clin. Invest.* **2003**, *112*, 1821−1830.
(28) Zhao, G.; Hochwalt, P. C.; Usui, M. L.; Underwood, R. A.; Singh, P. K.; James, G. A.; Stewart, P. S.; Fleckman, P.; Olerud, J. E. Delayed wound healing in diabetic (db/db) mice with Pseudomonas aeruginosa biofilm challenge: a model for the study of chronic wounds. *Wound Repair Regen.* **2010**, *18*, 467−477.
(29) Evrard, M.; Kwok, I. W. H.; Chong, S. Z.; Teng, K. W. W.; Becht, E.; Chen, J.; Sieow, J. L.; Penny, H. L.; Ching, G. C.; Devi, S.; Adrover, J. M.; Li, J. L. Y.; Liong, K. H.; Tan, L.; Poon, Z.; Foo, S.; Chua, J. W.; Su, I.-H.; Balabanian, K.; Bachelerie, F.; Biswas, S. K.; Larbi, A.; Hwang, W. Y. K.; Madan, V.; Koeffler, H. P.; Wong, S. C.; Newell, E. W.; Hidalgo, A.; Ginhoux, F.; Ng, L. G. Developmental Analysis of Bone Marrow Neutrophils Reveals Populations Specialized in Expansion, Trafficking, and Effector Functions. *Immunity* **2018**, *48*, 364−379.
(30) Matica, M. A.; Aachmann, F. L.; Tøndervik, A.; Sletta, H.; Ostafe, V. Chitosan as a Wound Dressing Starting Material: Antimicrobial Properties and Mode of Action. *Int. J. Mol. Sci.* **2019**, *20*, 5889.

https://doi.org/10.1021/acsbiomedchemau.1c00063
ACS Bio Med Chem Au 2022, 2, 409−418

(31) Jhunjhunwala, S.; Raimondi, G.; Thomson, A. W.; Little, S. R. Delivery of Rapamycin to Dendritic Cells Using Degradable Microparticles. *J. Controlled Release* **2009**, *133*, 191−197.
(32) Weichhart, T.; Hengstschläger, M.; Linke, M. Regulation of Innate Immune Cell Function by MTOR. *Nat. Rev. Immunol.* **2015**, *15*, 599−614.
(33) Raghavan, J. V.; Sagar, S. K.; Dorai, V. K.; Samuel, R. D.; Arunachalam, P.; Chaluvanarayana, H. C.; Belahalli, P.; Kalpana, S. R.; Jhunjhunwala, S. Biochemical and Immunological Predictors of Non-Healing in Individuals with Early-Stage Diabetic Foot Ulcers. Nov 11, **2021**. medRxiv:21266108 (accessed: Feb 13, 2022).
(34) Michaels, J.; Churgin, S. S.; Blechman, K. M.; Greives, M. R.; Aarabi, S.; Galiano, R. D.; Gurtner, G. C. db/dbmice exhibit severe wound-healing impairments compared with other murine diabetic strains in a silicone-splinted excisional wound model. *Wound Repair Regen.* **2007**, *15*, 665−670.
(35) Everett, E.; Mathioudakis, N. Update on management of diabetic foot ulcers. *Ann. N.Y. Acad. Sci.* **2018**, *1411*, 153−165.
(36) Laiva, A. L.; O'Brien, F. J.; Keogh, M. B. Innovations in Gene and Growth Factor Delivery Systems for Diabetic Wound Healing. *J. Tissue Eng. Regener. Med.* **2018**, *12*, e296−e312.
(37) Kasiewicz, L. N.; Whitehead, K. A. Recent Advances in Biomaterials for the Treatment of Diabetic Foot Ulcers. *Biomater. Sci.* **2017**, *5*, 1962−1975.
(38) Patel, S.; Srivastava, S.; Singh, M. R.; Singh, D. Mechanistic Insight into Diabetic Wounds: Pathogenesis, Molecular Targets and Treatment Strategies to Pace Wound Healing. *Biomed. Pharmacother.* **2019**, *112*, 108615.
(39) Wang, B.; Chandrasekera, P.; Pippin, J. Leptin- and Leptin Receptor-Deficient Rodent Models: Relevance for Human Type 2 Diabetes. *Curr. Diabetes Rev.* **2014**, *10*, 131−145.
(40) Zhang, H.; Yang, Z.; Zhang, W.; Niu, Y.; Li, X.; Qin, L.; Su, Q. White Blood Cell Subtypes and Risk of Type 2 Diabetes. *J. Diabetes Complicat.* **2017**, *31*, 31−37.
(41) Xie, X.; Shi, Q.; Wu, P.; Zhang, X.; Kambara, H.; Su, J.; Yu, H.; Park, S.-Y.; Guo, R.; Ren, Q.; Zhang, S.; Xu, Y.; Silberstein, L. E.; Cheng, T.; Ma, F.; Li, C.; Luo, H. R. Single-Cell Transcriptome Profiling Reveals Neutrophil Heterogeneity in Homeostasis and Infection. *Nat. Immunol.* **2020**, *21*, 1119−1133.
(42) Alakesh, A.; Jothiprakasam, T.; Raghavan, J. V.; Jhunjhunwala, S. Sterile Inflammation Alters Neutrophil Kinetics in Mice. *J. Leukoc. Biol.* **2022**, DOI: 10.1002/JLB.1A0321-132RR.
(43) Strydom, N.; Rankin, S. M. Regulation of Circulating Neutrophil Numbers under Homeostasis and in Disease. *J. Innate Immun.* **2013**, *5*, 304−314.
(44) Martin, C.; Burdon, P. C. E.; Bridger, G.; Gutierrez-Ramos, J.-C.; Williams, T. J.; Rankin, S. M. Chemokines Acting via CXCR2 and CXCR4 Control the Release of Neutrophils from the Bone Marrow and Their Return Following Senescence. *Immunity* **2003**, *19*, 583−593.
(45) Zhu, S.; Yu, Y.; Ren, Y.; Xu, L.; Wang, H.; Ling, X.; Jin, L.; Hu, Y.; Zhang, H.; Miao, C.; Guo, K. The Emerging Roles of Neutrophil Extracellular Traps in Wound Healing. *Cell Death Dis.* **2021**, *12*, 984.
(46) Diegelmann, R. F. Excessive Neutrophils Characterize Chronic Pressure Ulcers. *Wound Repair Regen.* **2003**, *11*, 490−495.
(47) Wetzler, C.; Kämpfer, H.; Stallmeyer, B.; Pfeilschifter, J.; Frank, S. Large and Sustained Induction of Chemokines during Impaired Wound Healing in the Genetically Diabetic Mouse: Prolonged Persistence of Neutrophils and Macrophages during the Late Phase of Repair. *J. Invest. Dermatol.* **2000**, *115*, 245−253.
(48) Dowey, R.; Iqbal, A.; Heller, S. R.; Sabroe, I.; Prince, L. R. A Bittersweet Response to Infection in Diabetes; Targeting Neutrophils to Modify Inflammation and Improve Host Immunity. *Front. Immunol.* **2021**, *12*, 678771.
(49) Atashgah, R. B.; Ghasemi, A.; Raoufi, M.; Abdollahifar, M.-A.; Zanganeh, S.; Nejadnik, H.; Abdollahi, A.; Sharifi, S.; Lea, B.; Cuerva, M.; Akbarzadeh, M.; Alvarez-Lorenzo, C.; Ostad, S. N.; Theus, A. S.; LaRock, D. L.; LaRock, C. N.; Serpooshan, V.; Sarrafi, R.; Lee, K.-B.; Vali, H.; Schönherr, H.; Gould, L.; Taboada, P.; Mahmoudi, M. Restoring Endogenous Repair Mechanisms to Heal Chronic Wounds with a Multifunctional Wound Dressing. *Mol. Pharm.* **2021**, *18*, 3171−3180.
(50) Vézina, C.; Kudelski, A.; Sehgal, S. N. Rapamycin (AY-22,989), a New Antifungal Antibiotic. I. Taxonomy of the Producing Streptomycete and Isolation of the Active Principle. *J. Antibiot.* **1975**, *28*, 721−726.
(51) Gomez-Cambronero, J. Rapamycin inhibits GM-CSF-induced neutrophil migration. *FEBS Lett.* **2003**, *550*, 94−100.
(52) Dunn, J. L. M.; Kartchner, L. B.; Gast, K.; Sessions, M.; Hunter, R. A.; Thurlow, L.; Richardson, A.; Schoenfisch, M.; Cairns, B. A.; Maile, R. Mammalian Target of Rapamycin Regulates a Hyperresponsive State in Pulmonary Neutrophils Late after Burn Injury. *J. Leukoc. Biol.* **2018**, *103*, 909−918.
(53) McInturff, A. M.; Cody, M. J.; Elliott, E. A.; Glenn, J. W.; Rowley, J. W.; Rondina, M. T.; Yost, C. C. Mammalian target of rapamycin regulates neutrophil extracellular trap formation via induction of hypoxia-inducible factor 1 α. *Blood* **2012**, *120*, 3118−3125.
(54) Lin, H. Y.-H.; Chang, K.-T.; Hung, C.-C.; Kuo, C.-H.; Hwang, S.-J.; Chen, H.-C.; Hung, C.-H.; Lin, S.-F. Effects of the MTOR Inhibitor Rapamycin on Monocyte-Secreted Chemokines. *BMC Immunol.* **2014**, *15*, 37.
(55) Li, J.; Kim, S. G.; Blenis, J. Rapamycin: One Drug, Many Effects. *Cell Metab.* **2014**, *19*, 373−379.
(56) Ballou, L. M.; Lin, R. Z. Rapamycin and MTOR Kinase Inhibitors. *J. Biol. Chem.* **2008**, *1*, 27−36.
(57) Ahmed, A.; Getti, G.; Boateng, J. Medicated Multi-Targeted Alginate-Based Dressings for Potential Treatment of Mixed Bacterial-Fungal Infections in Diabetic Foot Ulcers. *Int. J. Pharm.* **2021**, *606*, 120903.